

DYNAMICS OF MUTUALLY COUPLED THOMAS OSCILLATORS WITH LINEAR AND NONLINEAR COUPLING AND SWARMING

Vinesh Vijayan & Biplab Ganguli
Department of Physics & Astronomy
National Institute of Technology
Rourkela, Odisha-769008, India
513PH3005@nitrkl.ac.in & biplabg@nitrkl.ac.in
J.Clinton Sprott
Emeritus Professor of Physics
University of Wisconsin, 1150 University Avenue
Madison, WI 53706-1390 USA
sprott@physics.wisc.edu

October 27, 2022

Abstract

We consider two identical chaotic Thomas oscillators, mutually coupled with linear and sinusoidal non-linear coupling functions. Nature of dynamics and synchronization properties are studied for two qualitatively different regions of system parameters, $b(= 0.18 \text{ \& } 0.1998)$. Though uncoupled oscillator does not go through transient state, the coupled system passes through transient chaos or limit cycle before it settles to a chaotic or limit cycle attractor. Limit cycle attractor appears for low coupling in all the cases, when they are not synchronized or weakly synchronized. When they are coupled with sinusoidal nonlinear coupling, the coupled system bifurcates to complete synchronized chaotic state from space synchronized long transient limit cycle for higher values of coupling for $b = 0.18$. In the case of $b = 0.1998$, the coupled system settles either to synchronized chaotic or space synchronized limit cycle attractor depending on initial condition beyond a higher critical value of coupling constant. This shows there exists multistable states for $b = 0.1998$ for higher value of coupling constant. The nature of synchronization is complete synchronization when attractor is chaotic, even for unstable transient attractor, but it is either lag, anti-lag or space lag when the attractor is a limit cycle. For a nonlinearly coupled system, a full form of non-linear stability theory is applied instead of linear form.

1 Introduction

The interface of Nonlinear science, Statistical physics and computation is an avenue of exploring and analyzing man-made or naturally occurring complex systems. Complex systems, often containing more than one individual unit, are open systems which interact among themselves as well as with the environment in a linear/nonlinear way to produce some new behaviors(emergent behaviors), such as synchronization, chimera states, amplitude death, swarming etc, which the individual does not possess. The process of achieving this new behavior is known as self-organization. When the individual parts of the system interact among themselves as well as with the environment many new dynamical features start to manifest such as multistability, transient chaos, etc. Whether natural or artificial, the complex system interacts in a way to extrimize certain processes such that it may be trying to transport, dissipate and distribute energy in an efficient manner.

Traditionally chaos is a long-term asymptotic property which lives for, from a physical point of view, time scales much larger than the largest observational time scales. But there exist chaotic phenomena with finite life span and is known as transient chaos such that the time scales are shorter than the largest observational time. Such phenomena are interesting and relevant in many applications[1][2][3][4][5] [6][7][8][9][10] [11]. Depending upon the initial conditions these transients live for different times in different systems[1][12][13]. These transient states are examples for a nonequilibrium state which is different from the asymptotic state. Wherever transient chaos is observed the system moves around chaotically and then suddenly jumps to a steady-state, which is different than the transients. For example, with stirred chemical reactions in a closed container, it has been shown experimentally and theoretically that one can observe long-lasting chaotic transients with sufficiently nonequilibrium initial conditions[14][15]. Diffusion of particles along a given direction, just like in the case of active Brownian motion in a fluid can be analyzed and interpreted as a consequence of transient chaos together with other transport phenomena. The directed motion of particles, in this case, can be seen as a synchronization process[1].

The recent attraction of research which evoked much curiosity among researchers working on synchronization is about swarmalators - oscillators that move through space without changing their internal dynamics but move co-operatively when coupled as opposed to laser arrays or cardiac pacemaker cells[16]. These are oscillators whose phases affect their dynamics. Experiments have shown that the dynamics of phase is controlled by the number of nearby oscillators and bidirectional coupling between spatial and phase dynamics and is a necessary condition for swarmalators. This was observed for a population of bacteria whose internal dynamics were cyclically symmetric[17].

Rene Thomas proposed a particularly simple 3D flow which produces remark-

able dynamical behavior and became a prototype for chaos studies[18]. The model is given by

$$\begin{aligned}\frac{dx}{dt} &= -bx + \sin y \\ \frac{dy}{dt} &= -by + \sin z \\ \frac{dz}{dt} &= -bz + \sin x\end{aligned}\tag{1}$$

This model represents a particle moving in a force field with frictional damping under the action of some external source of energy. Two important characteristics of this system need more attention. One is the symmetry under the cyclic interchange of x, y, z co-ordinates and the other is the sole parameter b which is the damping coefficient. Originally it was developed as a model for a feedback circuit[18]. Theoretical models based on feedback circuits are useful to understand phenomena of many real systems like cell differentiation[19] and regulatory network[20]. In general, this system is suitable for mathematical modeling of biological systems[21]. Recently formation of Chimera states in a network of linearly and non-linearly coupled hundred Thomas oscillators is also studied[22].

Figure(1) shows the bifurcation and Lyapunov spectrum as a function of b . The system varies smoothly from a chaotic dissipative system to a chaotic conservative system and the latter case provides the only example for fractional diffusion in a purely deterministic system[18]. In the limit $b = 0$, the system can perform a chaotic walk. Route to chaos and its symbolic dynamics are well-studied problems [23][24].

Despite the richness in dynamics of the Thomas system, and its possible applications in many real systems discussed above, there is no study on the synchronization properties of the coupled Thomas systems. Therefore the detailed study of two coupled Thomas oscillators may facilitate quantitative understanding of real systems especially the process of swarming and directed motion. Brownian motion can also be seen as active unit motion, where the active unit has random fluctuation or is closely related to chaotic motion. Active motion is associated with internal energy through velocity-dependent friction[25]. Thus depending on the frictional term, the parameter b plays the role of absorbing or releasing energy. Therefore it sets a self- driven active motion in the presence of an environment. There is a recent study of collective motion of active Brownian particles with polar alignment. The system was modeled with stochastic dynamics with non-linear phase coupling[26]. Understanding of collective dynamics of two or more active units will lead to a better understanding of the collective motion of Brownian particles in biological systems and in general collective dynamics of large ensembles of interacting active particle units[25]. This lays the importance of the study of synchronization of coupled Thomas oscillators.

Therefore the motivation is to quantify the collective dynamics and explore

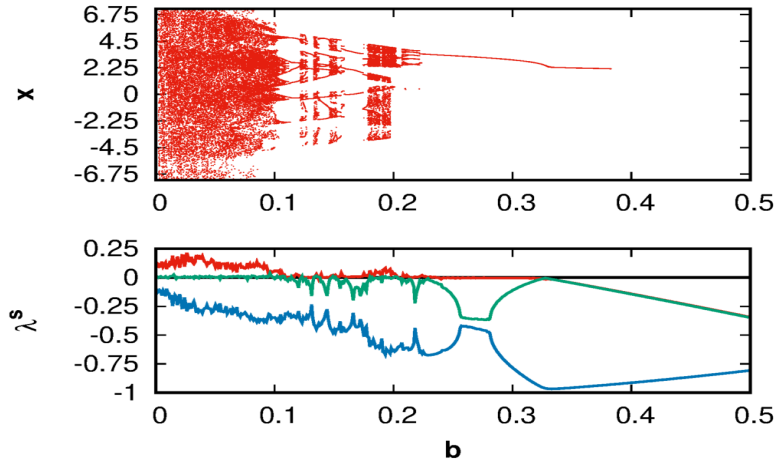


Figure 1: Bifurcation and Lyapunov spectrum for Thomas oscillator

collective behavior of the Thomas oscillators using numerical simulation. Pattern like Chimera states is already explored in a network of non-linearly coupled hundred Thomas oscillators[22] which provides a possible model for the dynamics of active particles like Brownian motion. In the present paper we consider only two coupled identical Thomas oscillators under a mutual coupling scheme with linear and nonlinear coupling functions. Though the majority of studies consider linear coupling in chaotic systems, the non-linear coupling is general and more applicable to real systems[26]. Linear coupling function is applicable for an approximate case of the non-linear, like harmonic approximation. Master stability function(MSF) is also formulated only for the linear coupling. Since Thomas system has only one parameter and that also being a coefficient with linear term, the non-linear coupling constant provides one more parameter to control the dynamics. This is particularly important in the limit $b = 0$, when the system shows chaotic walk. For the synchronization studies we have chosen $b = 0.18$ and $b = 0.1998$ where we have stable chaotic oscillations but with a reasonable size of attractor unlike attractors of very large sizes for very low values of b . There is a difference in the size of the attractors such that the attractor at $b = 0.1998$ is just the one third the size of the attractor at $b = 0.18$ as we observe from the phase space plot. Moreover, the uncoupled dynamics do not show any transient chaos for these system parameter values. There is one more major difference between the systems with $b = 0.18$ and $b = 0.1998$. The dynamics in the latter case is such that the stable chaotic dynamics fall at the boundary of chaos and quasiperiodic oscillations. In this sense this value of b is also chosen for comparison purposes (Figure(1)). We call this regime as chaotic at the boundary of chaos and quasiperiodic. The dynamics of the coupled system are explained based on the largest Lyapunov exponent(LLE) and bifurcation

diagram. The stability of synchronization is analyzed by the largest transverse Lyapunov exponents(LTE), without any linearization in the case of nonlinear coupling. The onset of CS synchronization is verified by Pearson coefficient(ρ) and the transverse distance (TD) on the synchronization manifold. Synchronization thresholds are analyzed and compared for the two cases with linear as well as nonlinear coupling functions.

2 Mutually Coupled Thomas System and Transient Chaos

Two Thomas oscillators, coupled either linearly or non-linearly(sinusoidal), undergo a long period of transient unstable attractor, mainly chaotic before settling to a stable attractor. The transient period of time depends on the initial condition. Therefore with a suitable initial condition, the coupled system may be brought to a stable attractor within a short span of time. The period of transient chaos is longer in the case of $b = 0.1998$ than $b = 0.18$. This period gets further increased due to non-linear coupling.

Therefore in our study, different initial conditions are chosen to study transient states and to explore possible final asymptotic states. Three sets of initial conditions are applied. (i) The first one is what we call resetting. In this case, for each coupling constant, a fixed initial condition is used, and that is a point on the basin of attraction of the uncoupled oscillators. This case is equivalent to performing independent experiments on the same system with a fixed coupling element but of different values for subsequent experiments, keeping the initial condition the same. (ii) In the second case, the same initial condition is used as the first case for an uncoupled system. In the subsequent coupled system, the long-term solution of the previous coupled system is varied by 10% to be used as an initial condition for the next coupled system. This is done by varying the coupling constant by a step of δcc to achieve a new coupled system. (iii) In the third case, 1% variation is applied to the previous long-term solution for the next system. It is important to see how one can control these transients so that it can be used for practical purposes. The last two cases require a single experiment with a variable coupling element that can be varied during an experiment, like a variable resistor in a circuit. When the coupling element is varied, simultaneously one of the oscillators is slightly disturbed externally so that the initial condition for the new coupling is 10% or 1% different from the final state.

(Figure(2)) shows the transient chaos observed at the periodic(limit cycle) windows with the third set of initial conditions. For $b = 0.18$ with linear coupling and at $cc = 0.16$, we find the asymptotic state to be a limit cycle with transient time $5K$ of chaos(Figure(2-a)). With nonlinear coupling, at $cc = 0.12$, we observe transient chaos, and the asymptotic state is again a limit cycle corre-

sponding to complex oscillations but with transient time $25K$ (Figure(2-b)). In the case of $b = 0.1998$ with linear coupling, the asymptotic dynamics shows a window of limit cycle at $cc = 0.05$ with a chaotic transient time of $50K$ (Figure(2-c)). With nonlinear coupling and $cc = 0.41$, the transient time is $80K$ and the asymptotic final state is complex oscillations(Figure(2-d)).

3 Bidirectionally Coupled Thomas System With Linear Coupling

The mutual linear coupling is provided to the x variable. Since the system is symmetric with respect to interchange among all the variables, coupling to other variables instead to x would give the same dynamics.

The governing equation of motion is given by

$$\begin{aligned}\dot{x}_{1,2} &= -bx_{1,2} + \sin y_{1,2} + cc * (x_{2,1} - x_{1,2}) \\ \dot{y}_{1,2} &= -by_{1,2} + \sin z_{1,2} \\ \dot{z}_{1,2} &= -bz_{1,2} + \sin x_{1,2}\end{aligned}\tag{2}$$

where cc is the coupling coefficient.

In this case the final state does not depend on the initial condition showing the absence of multistable states. We chose the third set of choices for the initial condition for all the calculations as for this choice transient time is least.

3.0.1 Linear diffusive coupling with $b=0.18$

The dynamics of mutually coupled Thomas systems with $b = 0.18$ can be visualized from the Lyapunov spectra and bifurcation diagram, as shown in Figure(3). With the third set of initial condition, the nature of the dynamics is such that there is a transition from hyperchaotic to chaotic behaviour, indicated by the number of positive Lyapunov exponents, as we smoothly vary cc from zero to a sufficiently large value. The nature of dynamics also changes for a range of intermediate values of the coupling coefficient. There are limit cycle oscillations, as indicated by the zero value of the largest Lyapunov exponent(LLE)(red line) with all other being negative, in the range $cc \sim 0.11 - cc \sim 0.3$ with a small window of chaos which is confirmed by the positivity of the LLE(red line).

The stability of the synchronized manifold is given by the negativity of the largest transverse Lyapunov exponent, λ^\perp (LTE). LTE is calculated from the time evolution of the perturbation projections perpendicular to the synchronized manifold. Parallel and perpendicular projections of perturbations are defined by Equation(3) and their time evolutions are governed by Equation(4).

$$\delta\mathbf{X}_\parallel = (\delta\mathbf{x}_1 + \delta\mathbf{x}_2)/\sqrt{2} \quad \delta\mathbf{X}_\perp = (\delta\mathbf{x}_1 - \delta\mathbf{x}_2)/\sqrt{2}\tag{3}$$

$$\delta\dot{\mathbf{X}}_\parallel = \mathbf{J}(\mathbf{X}).\delta\mathbf{X}_\parallel \quad \delta\dot{\mathbf{X}}_\perp = [\mathbf{J}(\mathbf{X}) - 2\mathbf{C}].\delta\mathbf{X}_\perp\tag{4}$$

where $\mathbf{J}(\mathbf{X})$ is the Jacobian matrix evaluated at the synchronization manifold. \mathbf{C} is the coupling matrix given by

$$\mathbf{C} = cc \begin{bmatrix} 1 & 0 & 0 \\ 0 & 0 & 0 \\ 0 & 0 & 0 \end{bmatrix} \quad (5)$$

where cc is the coupling strength. The synchronization manifold is stable when the perturbations transversal to the manifold die out exponentially. This implies that all the Lyapunov exponents for the transversal perturbations are negative[27].

The system displays a transition to complete synchronized(CS) state, defined by $\mathbf{x}_1(t) = \mathbf{x}_2(t) = \mathbf{X}(t)$ at a critical value of cc_T . This is the only type of synchronized state-observed throughout the range of cc from the onset(critical) value. This transition is due to two counter-balancing effects. The instability of the synchronized manifold is measured by the LLE whereas the diffusion measures the stability. When diffusion dominates over instability, the system synchronizes and the motion takes place in an invariant subspace of synchronization manifold described by $\dot{\mathbf{X}}(t) = \mathbf{F}(\mathbf{X}(t))$. Detection of CS is observed by the calculation of Pearson coefficient(ρ), the degree of cross- correlation between the variables[28], defined by Equation(6).

$$\rho = \frac{\langle (\mathbf{x}_1 - \langle \mathbf{x}_1 \rangle)(\mathbf{x}_2 - \langle \mathbf{x}_2 \rangle) \rangle}{\sqrt{\langle (\mathbf{x}_1 - \langle \mathbf{x}_1 \rangle)^2 \rangle \langle (\mathbf{x}_2 - \langle \mathbf{x}_2 \rangle)^2 \rangle}} \quad (6)$$

where $\langle . \rangle$ denotes full space time average. The averages are calculated after the initial transients. When $\rho = 1$ the two variables are completely correlated, $\rho = -1$ means negatively correlated and for $\rho = 0$, the two variables are completely uncorrelated.

We rely on another important measure of the CS manifold, that is the average distance from the synchronized manifold $|x_{\perp}|_{rms}$ and its maximum observed values $|x_{\perp}|_{max}$. The former being sensitive to global stability while the latter to local stability[29]. It is defined by Equation(7).

$$|x_{\perp}|_{rms} = \lim_{T \rightarrow \infty} \frac{1}{T - T_0} \int_{T_0}^T |\mathbf{x}_1(\mathbf{t}) - \mathbf{x}_2(\mathbf{t})| d\mathbf{t} \quad (7)$$

where T_0 is the transient time and T , is the total time of computation.

From Figure(5), the threshold for CS is confirmed to be $cc_T \sim 0.49$ which is stable as indicated by the plot for TLE, Figure(4). From Figure(4), we also make the following observation that TLE is negative in the range $cc \sim 0.14 - cc \sim 0.3$ and $cc \sim 0.31 - cc \sim 0.43$ such that the former is well within the limit cycle region as observed from the Lyapunov spectra. They both correspond to weak forms of stable synchronization, which is indeed possible on the way to achieving CS. Figure(5) shows Pearson coefficient(ρ) and Transverse distance (TD) and agrees well with TLE.

The above picture of dynamics, as well as synchronization, is not affected by changing the initial condition. The only change due to different initial conditions is that in the survival time of transient chaos. In the present calculation, transient chaos persisted up to $T = 5K$ with 1% variation in the initial condition after every cycle of δcc . The important point to be noted here is that the synchronization is not affected by the transient states. The synchronized and desynchronized states are shown below in Figure(6).

3.0.2 Linear diffusive coupling with $b=0.1998$

The qualitative nature of dynamics, in this case, is similar to that of the previous case except for the fact that the small window of chaos has now been located at the middle of the limit cycle region in the range of $cc \sim 0.12 - 0.29$ indicated by LLE(red line) as shown in Figure(7).

As far as synchronization is concerned the threshold for CS has now been shifted towards the left with a value $cc_T \sim 0.33$. This shows that stable CS is achieved much earlier than that in the previous case and is confirmed by the LTE. Like in the previous case here also we have weak forms of synchronization in the range of limit cycle oscillations in the low range of cc . Figures(8, 9, 10) show synchronization for this case.

4 Bidirectionally Coupled Thomas System With Nonlinear Coupling

In the case of sinusoidal nonlinear bidirectional coupling, the dynamics is given by

$$\begin{aligned} \dot{x}_{1,2} &= -bx_{1,2} + \sin y_{1,2} + cc * \sin(x_{2,1} - x_{1,2}) \\ \dot{y}_{1,2} &= -by_{1,2} + \sin z_{1,2} \\ \dot{z}_{1,2} &= -bz_{1,2} + \sin x_{1,2} \end{aligned} \tag{8}$$

The dynamics of transverse perturbation, governed by the Equation(4) gets modified to (without any approximation (linearization))

$$\delta \dot{\mathbf{X}}_{\perp} = [J(\mathbf{X}) - 2 * C * \cos(x_2 - x_1)].\delta \mathbf{X}_{\perp} \tag{9}$$

4.0.1 Nonlinear diffusive coupling with $b = 0.18$

In this case one can immediately see the effect of nonlinear coupling compared to the linearly coupled case. The range of cc of the limit cycle oscillations now shifted to the left, $0.012 - 0.13$. The dynamics are such that there is a transition from hyperchaotic to chaotic behavior via limit cycle oscillations. Also, the small region of chaotic oscillations in the limit cycle region has now disappeared.

The Lyapunov spectra and bifurcation diagrams are shown in Figure(11). This is achieved by the third set of initial condition with transient time $25K$.

The threshold for complete synchronization, in this case, is found to be $cc_T = 0.46$, which is slightly less than that of the case with the linear coupling, and it is stable as indicated by LTE in Figure(12). The thresholds are shown in Figure(13). Before this transition, LTE becomes negative at a particular value of $cc = 0.05$, where LLE simultaneously just touches the zero value. This shows a weak form of synchronization, which is amplitude envelope synchronization(AES)[30]. But AES is extremely sensitive to the changes in coupling constant, as evident from the LTE spectrum.

With nonlinear coupling in effect, the second set of initial conditions and after a transient time of $25K$, we get the same picture of dynamics showing the asymptotic states as chaotic. Interesting transient phenomena is observed, when we look at the dynamics below the transient time, say $24K$, but still with 1% variation in the initial condition after every cycle of cc (third set of initial condition), shown in Figure(14). Here for lower values of cc , the dynamics are found to be almost the same as that of the $25K$ transient case. But at higher values of coupling coefficient, we have different dynamical behavior. Now beyond $cc = 0.61$ we have limit cycles. The synchronization property is calculated for this case with the Pearson coefficient and transverse distance, and we are getting an interesting result as shown in Figure(15).

From ρ and TD calculations, we note the following observations. There is CS in the range $cc = 0.46 - cc = 0.61$. After that, the CS is lost, but there exists a strong correlation between the variables as $\rho \approx 1$. Time series analysis for the range $cc = 0.61 - 1$ shows the oscillations in this range are spatially separated, or we can say there is a space lag. This spatial separation of oscillators with correlated time behaviour is known as swarming. The time series is shown in Figure(16)

This is indeed possible in the case of self-propelled active agents and also shows the richness of the transient phenomena. Similar result is found with second set of initial condition too.

4.0.2 Nonlinear diffusive coupling with $b = 0.1998$

Finally, we look at the synchronization properties of mutually coupled Thomas systems under sinusoidal coupling for $b = 0.1998$ with the third set of the initial condition. The dynamics are found to be different from the previous cases in that now we have two windows of limit cycle oscillations i.e. the dynamics become much more complex in this case. The two windows of limit cycle oscillations are $cc \sim 0.029 - cc \sim 0.059$ and $cc \sim 0.42 - cc \sim 0.46$. The final state achieved by the coupled system with 1% variation in the initial condition after every cycle of cc and transient time $80K$ is chaotic. The hyperchaotic nature of the coupled system persists much more longer here upto $cc = 0.23$ except for the

first window of limit cycle oscillation. The bifurcation diagram and Lyapunov spectra are shown in figure(17).

The CS threshold is around $cc_T \sim 0.35$ and is stable, as indicated by the LTE in Figure(18). In this case, there is only a single cut along the coupling axis on the way to stability. The Pearson coefficient and Transverse distances for this case are shown in Figure(19).

The phase portraits show the desynchronized state as well as the synchronized states for two different values of coupling coefficient, as shown in Figure(20).

In this case, we notice that in the second limit cycle range, that is, $cc = 0.42 - 0.46$ we do not have complete synchronization. To predict the nature of synchronization we choose a specific value in this range, say, $cc = 0.44$, and we analyze the time series. Figures(21) show there is indeed co-operative dynamics but not CS at these values of coupling. The synchronized states for $cc = 0.44$ seem to be either Lag Synchronization(LS) or Anti Lag Synchronization (ALS). To quantify and visualize the LS/ALS, we use the idea of similarity function[31]. The similarity function is defined as the time average of the variables $x_1(t)$ and $x_2(t + \tau)$. It is given by Equation(10). The LS can be seen by plotting $x_2(t + \tau)$ vs $x_1(t)$, Figure(21), and ALS by plotting $x_2(t - \tau)$ vs $x_1(t)$.

$$S_{\mp}^2 = \frac{\langle (x_2(t + \tau) \mp x_1(t))^2 \rangle}{\sqrt{\langle x_1^2(t) \rangle \langle x_2^2(t) \rangle}} \quad (10)$$

Our calculation with, second choice of initial condition shows that synchronized state after the critical value of $cc = 0.59$ is a stable limit cycle instead of chaos, shown in the bifurcation diagram(figure(22)). The limit cycle occupies largely in different regions in the phase space than the transient chaotic attractor as shown in figure(23). This shows the existence of multistable state.

The transient for both the initial conditions is taken as 80K, which is much higher compared to $b = 0.18$ case. The transient chaos lasts nearly 80K in the case of the third choice of initial condition throughout the range of cc . Whereas comparing the figures(22) and (17) it shows transient chaos lasts beyond 80K for low and intermediate values of cc but dies much earlier for a higher value when the final state is a limit cycle in the case of the second set initial condition.

To check the synchronized state, we calculated the synchronization measures up to the transient time 150K. Then also we got the final state to be limit cycle state with the nature of synchronization as space lag, means swarming. This lead us to remove the transient up to 150K. The asymptotic state remains to be a limit cycle but with no change in synchronization. Now also the system show swarming. So, we conclude that the synchronization, that we obtained at 80K,

is an asymptotic synchronization. Like in the previous cases, the synchronized state, when the dynamics is a limit cycle, is lag instead of CS. This clearly shows bifurcation from chaos to limit cycle changes the nature of synchronization from CS to LS / ALS or swarming.

Comparing the results for the two coupling schemes, it is clear that non-linearity in coupling function adds extra features in synchronized states. It is known that there is a bifurcation from CS to desynchronization for a higher value of coupling constant in two linearly coupled Rössler oscillators. This is because the master stability function cuts at two points on the coupling axis. But this is not the case here for non-linear coupling. In this case, master stability function predicts CS throughout, after the onset value of cc , which is verified from the result of linear coupling. This prediction is not obeyed in the case of non-linear coupling. The reason for this can be understood, based on the stability dynamics of the synchronized manifold given by equations (4) and (9) respectively. The Equation(4) is linear whereas Equation(9) is non-linear. In other words, Equation(4) is the linearized form of Equation(9). The master stability function is based on linearization of the Jacobian matrix. The linearization of Equation(9) will lead to a similar result as that of Equation(4), which does not capture a complete picture due to the presence of non-linear *cosine* term. Therefore we carried out a full calculation of the Lyapunov exponent instead of finding eigenvalues of the linearized Jacobian. Therefore we can capture the extra effects coming from nonlinear stability equations for synchronization. It is because of this small nonlinearity that gives rise to dramatic effect to produce bifurcation from CS to LS or ALS and also to CS(in the case of multistable case) at some intermediate value which is not captured by linear master stability function. The LS and ALS are otherwise known to be observed in linearly coupled autonomous non-identical chaotic oscillators, identical autonomous oscillators with delay coupling[28] or linearly coupled identical non-autonomous oscillators[32]. In all the previous cases LS and ALS appear before the onset of CS only. In the present case these two forms of synchronizations are observed between two stable CS or after CS.

Appearance of a weak form of synchronization before the onset of CS is due to the specific characteristics of the system, because it is observed for both linear and non-linear couplings.

5 Conclusion

Although there are no transient attractors in uncoupled Thomas oscillators, they appear (mostly transient chaos) when two oscillators are mutually coupled with either linear or nonlinear couplings. The lifetime of the transient state increases if the nature of the coupling is changed from linear to sinusoidal non-linear and it also increases with $b = 0.1998$, keeping the same initial condition.

Transient time depends on the initial condition. The coupled system bifurcates from transient chaos to asymptotic limit cycle for some window of low coupling in all the cases considered in this study. In this window of low coupling values, the coupled system does not achieve complete synchronization(CS), but shows a weak form of synchronization in some cases. The onset of CS occurs for lower coupling constant in the case of $b = 0.1998$ than $b = 0.18$. Both fall in the intermediate range. CS is achieved during transient chaotic state and remains so for final asymptotic chaotic state. In the case of $b = 0.18$, with nonlinear coupling, there is a limit cycle transient state throughout the higher values of coupling constant, slightly beyond the onset of CS. During this period of transient, coupled system is in a “space-lag synchronized state”(swarming-spatially separated with correlated time behaviour). The transient time persists for long before it bifurcates to a stable chaotic CS state. Unlike the case of $b = 0.18$, the non-linearly coupled system for $b = 0.1998$ bifurcates also from transient chaos to stable limit cycle for some small window of coupling in the intermediate range but beyond the onset of CS. In this limit cycle state, oscillators show time lag synchronization. There is no transient to limit cycle for coupling far from onset of CS. System for one set of initial conditions remains chaotic in CS state for higher value of coupling. But for some other set of initial conditions the system settles to an asymptotic limit cycle for the same higher value of coupling but in space lag synchronized state. This limit cycle attractor occupies different regions in phase space than the chaotic asymptotic state for the other initial condition. This shows the existence of multi-stable synchronized states in the case of $b = 0.1998$ with nonlinear coupling.

LS and ALS are earlier known to exist before achieving CS by linearly coupled non-identical or non-autonomous oscillators or time delay coupling. We are now, for the first time, able to achieve LS or ALS between stable CS in coupled identical oscillators by non-linear coupling and applying full non-linear stability theory. LS and ALS are confirmed by the calculations of similarity function and bifurcation diagram. Similar to linear case, in this case also a weak form of synchronization(amplitude envelope) is observed for very weak coupling where systems remain in chaotic regime for $b = 0.18$. Our result is very significant to understand collective motion of active units in a medium, like coupled Brownian particles. In such systems, there is a velocity-velocity correlation. Therefore variables in our model represent components of velocity. There is indeed a possibility of phase correlation (LS or ALS) among the velocities of Brownian particles other than moving with common velocity(CS). In the context of collective motion of Brownian particles, CS means absorbing/releasing energy from/ to source (medium) simultaneously. Whereas LS with a phase difference of π would mean that when one particle releases energy, the other absorbs at the same time, as if no energy transfers to / from the source. This is indeed possible in Brownian motion.

Study of synchronization property of two coupled Thomas oscillators is the first step to understand phenomena in many real systems. The stochastic dynamics of Brownian motion can also be modeled with Chaotic dynamics of Thomas sys-

tem. A full understanding of collective motion of active units can be achieved when we consider co-operative dynamics of large units. Extension of the present study to include large units provides a clear picture of patterns like chimera or cluster states.

In this study, we are able to produce different results not observed earlier. Like synchronization does not get affected by transient state in all the cases when asymptotic state is also a chaotic trajectory. When there is a transition from transient chaos to asymptotic limit cycle, there is a change in nature of synchronization as observed in the case of $b = 0.1998$ with nonlinear coupling. Appearance of lag / anti-lag synchronizations and swarming within the regime of complete synchronization, and transient limit cycle to chaos is due to non-linear coupling.

References

References

- [1] Y.-C. Lai, T. Tél, *Transient Chaos*, Applied Mathematical Sciences, Springer, 2011.
- [2] D. Dangoisse, P. Glorieux, D. Hennequin, Laser chaotic attractors in crisis, *Physical Review Letters* 57 (1986) 2657 – 2660. doi:<https://doi.org/10.1103/physrevlett.57.2657>.
- [3] K. Mccann, P. Yodzis, Bifurcation structure of a three-species food-chain model, *Theoretical Population Biology* 28 (1995) 93 – 125. doi:<https://doi.org/10.1006/tpbi.1995.1023>.
- [4] M. Dhamala, Y.-C. Lai, Controlling transient chaos in deterministic flows with applications to electrical power systems and ecology, *Physical Review E* 59 (1999) 1646 – 1655. doi:<https://doi.org/10.1103/physreve.59.1646>.
- [5] Z. T. Mária Ercsey-Ravasz, Optimization hardness as transient chaos in an analog approach to constraint satisfaction, *Nature Physics* 7 (2011) 966 – 970. doi:<https://doi.org/10.1038/nphys2105>.
- [6] R. Sumi, B. Molnár, M. Ercsey-Ravasz, Robust optimization with transiently chaotic dynamical systems, *Europhysics Letters* 106 (2014) 40002. doi:<https://doi.org/10.1209/0295-5075/106/40002>.
- [7] Z. T. Mária Ercsey-Ravasz, The chaos within sudoku, *Scientific Reports* 2. doi:<https://doi.org/10.1038/srep00725>.
- [8] T. Haszpra, T. Tél, Escape rate: a lagrangian measure of particle deposition from the atmosphere, *Nonlinear Processes in Geophysics* 20 (2013) 867 – 881. doi:<https://doi.org/10.5194/npg-20-867-2013>.

- [9] T. Haszpra, , A. Horányi, Some aspects of the impact of meteorological forecast uncertainties on environmental dispersion prediction, Quarterly Journal of the Hungarian Meteorological Service 118 (2014) 335–347. doi:<https://doi.org/10.28974/idojaras.2018.2.1>.
- [10] T. Haszpra, T. Tél, Topological entropy: A lagrangian measure of the state of the free atmosphere, Journal of the Atmospheric Sciences 70 (2013) 4030 – 4040. doi:<https://doi.org/10.1175/jas-d-13-069.1>.
- [11] A. E. Motter, M. Gruiz, G. Károlyi, T. Tél, Doubly transient chaos: Generic form of chaos in autonomous dissipative systems, Physical Review Letters 111 (2013) 94101. doi:<https://doi.org/10.1103/physrevlett.111.194101>.
- [12] T. Tél, The joy of transient chaos, Chaos: An Interdisciplinary Journal of Nonlinear Science 25 (2015) 097619. doi:<https://doi.org/10.1063/1.4917287>.
- [13] R. Capeáns, J. Sabuco, M. A. F. Sanjuán, J. A. Yorke, Partially controlling transient chaos in the lorenz equations, Philosophical Transactions of the Royal Society A: Mathematical, Physical and Engineering Sciences 375 (2017) 20160211. doi:<https://doi.org/10.1098/rsta.2016.0211>.
- [14] S. K. Scott, B. Peng, A. S. Tomlin, K. Showalter, Transient chaos in a closed chemical system, The Journal of Chemical Physics 94 (1991) 1134–1140. doi:<https://doi.org/10.1063/1.460019>.
- [15] J. Wang, P. G. Soerensen, F. Hynne, Transient period doublings, torus oscillations, and chaos in a closed chemical system, The Journal of Chemical Physics 98 (1994) 725 – 727. doi:<https://doi.org/10.1021/j100054a001>.
- [16] K. P. O’Keefe, H. Hong, S. H. Strogatz, Oscillators that sync and swarm, Nature Communications 8. doi:<https://doi.org/10.1038/s41467-017-01190-3>.
- [17] O. A. Igoshin, A. Mogilner, R. D. Welch, D. Kaiser, G. Oster, Pattern formation and traveling waves in myxobacteria: Theory and modeling, Proceedings of the National Academy of Sciences 98 (2001) 14913 – 14918. doi:<https://doi.org/10.1073/pnas.221579598>.
- [18] R. Thomas, Deterministic chaos seen in terms of feedback circuits: Analysis, synthesis, ”labyrinth chaos”, Int. J. Bifurc. Chaos. 9 (1999) 1889–1905. doi:<https://doi.org/10.1142/S0218127499001383>.
- [19] R. Thomas, M. Kaufman, Multistationarity, the basis of cell differentiation and memory: I and ii, Chaos 11 (2001) 170–195. doi:<https://doi.org/10.1063/1.1350439> <https://doi.org/10.1063/1.1349893>.

- [20] R. Thomas, D. Thieffry, M. Kaufman, Dynamical behaviour of biological regulatory networks. i. biological role of feedback loops and practical use of concept of the loop-characteristics state, *Bull. Math Bio.* 57 (1995) 247–276. doi:<https://doi.org/10.1007/BF02460618>.
- [21] V. Basios, C. G. Antonopoulos, Hyperchaos and labyrinth chaos: Revisiting thomas–rössler systems, *Journal of Theoretical Biology* 460 (2019) 153–159. doi:<https://doi.org/10.1016/j.jtbi.2018.10.025>.
- [22] V. Vijayan, B. Ganguli, Pattern in nonlinearly coupled network of identical thomas oscillators, *Communication in Non-linear Science and Numerical Simulations* 99 (2021) 105819. doi:<https://doi.org/10.1016/j.cnsns.2021.105819>.
- [23] J. C. Sprott, K. E. Chlouverakis, Labyrinth chaos, *Int. J. Bifurc. Chaos.* 17 (2007) 2097–2108. doi:<https://doi.org/10.1142/s0218127407018245>.
- [24] G. Rowlands, J. C. Sprott, A simple diffusion model showing anomalous scaling, *Physics of Plasmas* 15 (2008) 082308. doi:<https://doi.org/10.1063/1.2969429>.
- [25] P. Romanczuk, M. Bär, W. Ebeling, B. Lindner, L. S. Geier, Active brownian particles, *Eur. Phys. J. Special Topics* 202 (2012) 1 – 162. doi:<https://doi.org/10.1140/epjst/e2012-01529-y>.
- [26] A. Martín-Gómez, D. Levis, A. Díaz-Guilera, I. Pagonabarraga, Collective motion of active brownian particles with polar alignment, *Soft Matter* 14 (2018) 2610 – 2618. doi:<https://doi.org/10.1039/c8sm00020d>.
- [27] H. Fujisaka, T. Yamada, Stability theory of synchronized motion in coupled-oscillator systems, *Prog.Theor.Phys.* 69 (1983) 32–47. doi:<https://doi.org/10.1143/ptp.69.32>.
- [28] J. M. González-Miranda, *Synchronization and Control of Chaos*, Imperial College Press, London, 2004.
- [29] D. J. Gauthier, J. C. Bienfang, Intermittent loss of synchronization in coupled chaotic oscillators: Toward a new criterion for high-quality synchronization, *Phys. Rev. Lett.* 77 (1996) 1751 – 1754. doi:<https://doi.org/10.1103/physrevlett.77.1751>.
- [30] J. M. Gonzalez-Miranda, Amplitude envelope synchronization in coupled chaotic oscillators, *Phys. Rev. E.* 65 (2002) 036232. doi:<https://doi.org/10.1103/physreve.65.036232>.
- [31] M. G. Rosenblum, A. S. Pikovsky, J. Kurths, From phase to lag synchronization in coupled chaotic oscillators, *Phys. Rev. Lett.* 78 (1997) 4193 – 4196. doi:<https://doi.org/10.1103/physrevlett.78.4193>.

- [32] S. Satpathy, B. Ganguli, Transition to complete synchronization of two diffusively coupled chaotic parametrically excited pendula, *Nonlinear Dynamics* 88 (2017) 2063–69. doi:[https://10.1007/s11071-017-3362-z](https://doi.org/10.1007/s11071-017-3362-z).

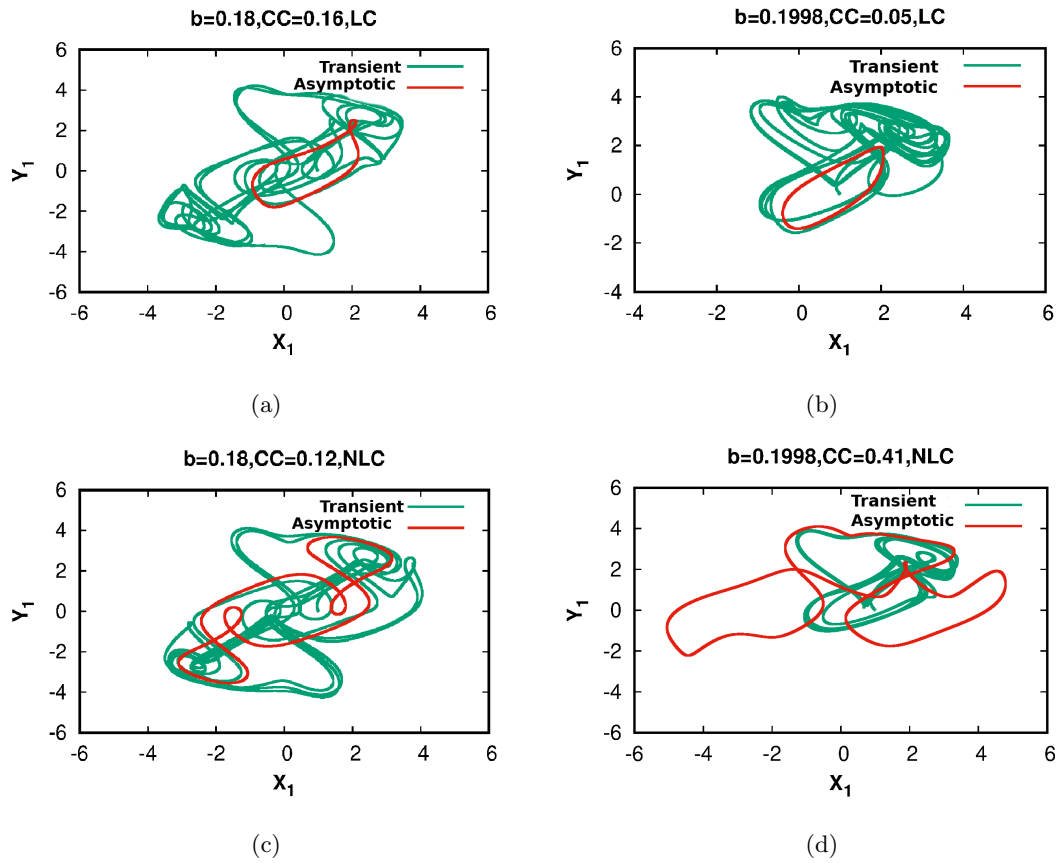


Figure 2: Plots showing transient chaos (green) and stable attractor (red) for linear (LC) and nonlinear (NLC) coupling for the choice of parameter values 0.18 and 0.1998 with specified coupling coefficients

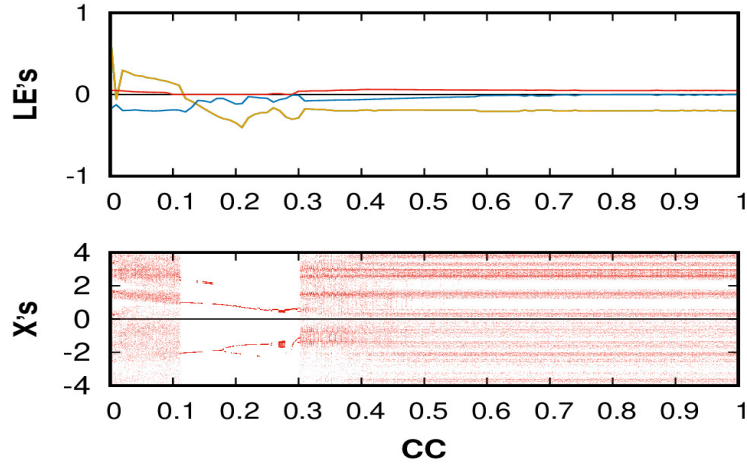


Figure 3: Lyapunov spectra and bifurcation diagram for the mutually coupled Thomas system with linear diffusive coupling with $b = 0.18$ (stable chaotic oscillations)

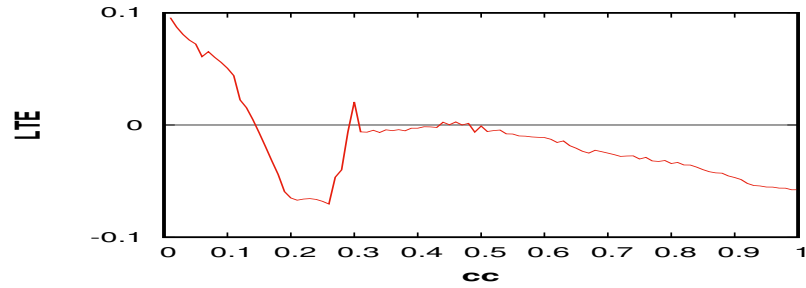


Figure 4: Transverse Lyapunov exponent λ^\perp (LTE) for the mutually coupled Thomas system with linear diffusive coupling with $b = 0.18$ (stable chaotic oscillations)

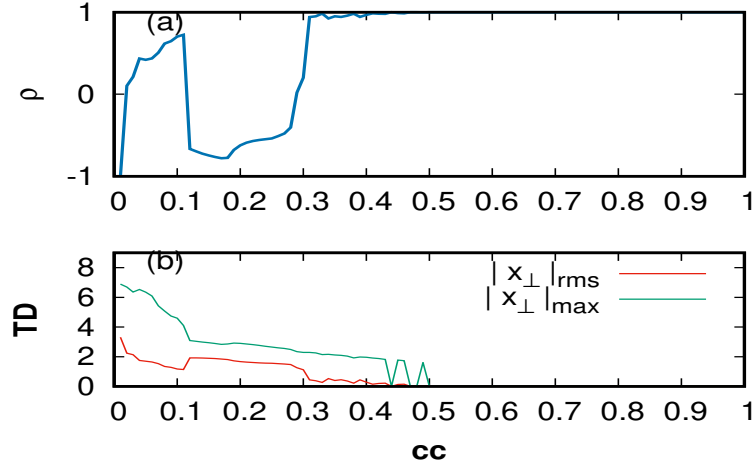


Figure 5: Pearson coefficient (ρ) and Transverse distance (TD) plot for the mutually coupled Thomas system with linear diffusive coupling with $b = 0.18$ (stable chaotic oscillations)

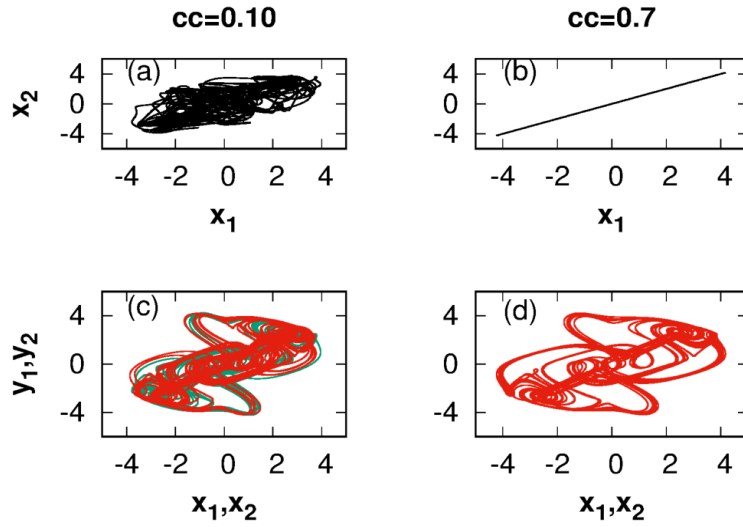


Figure 6: Phase portrait in the case of Linear Coupling(LC) with $b = 0.18$ for two different values of coupling coefficient. Desynchronized state (left panel) and synchronized state(right panel)

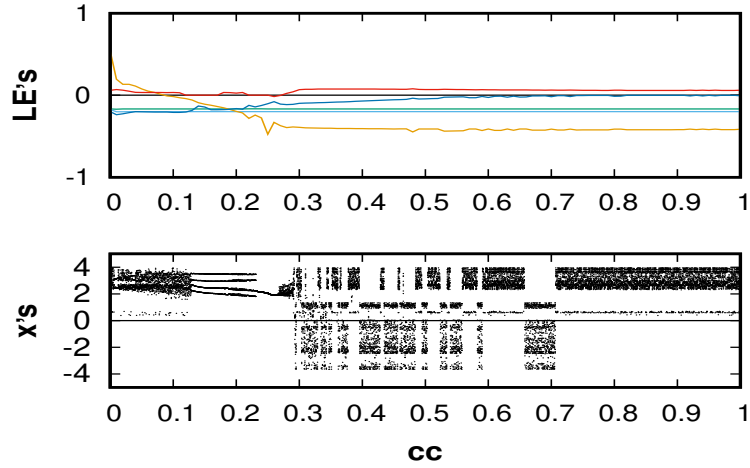


Figure 7: Lyapunov spectra and bifurcation diagram for the mutually coupled Thomas system with linear diffusive coupling with $b = 0.1998$ (chaotic oscillations at the boundary of chaos and quasi-periodic)

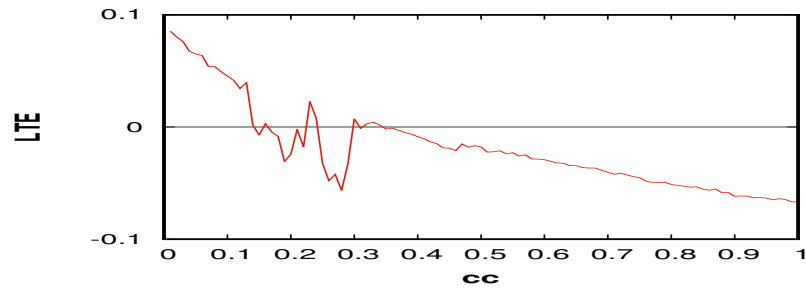


Figure 8: Transverse Lyapunov exponent λ^\perp (LTE) for the mutually coupled Thomas system with linear diffusive coupling with $b = 0.1998$ (chaotic oscillations at the boundary of chaos and quasi-periodic)

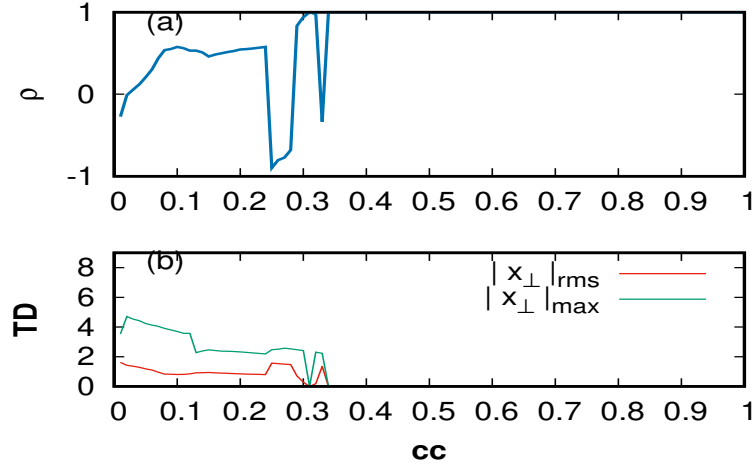


Figure 9: Pearson coefficient (ρ) and Transverse distance (TD) plot for the mutually coupled Thomas system with linear diffusive coupling with $b = 0.1998$ (chaotic cillations at the boundary of chaos and quasi-periodic)

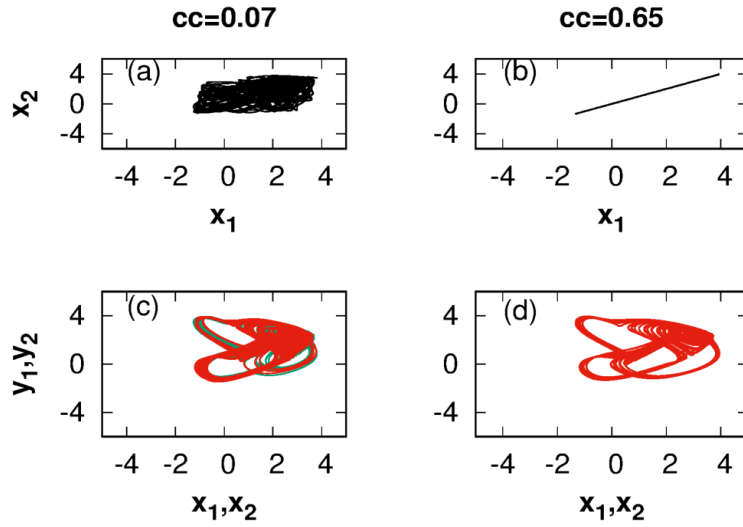


Figure 10: Phase portrait in the case of Linear Coupling(LC) with $b = 0.1998$ for two different values of coupling coefficient. Desynchronized state(left panel) and synchronized state(right panel)

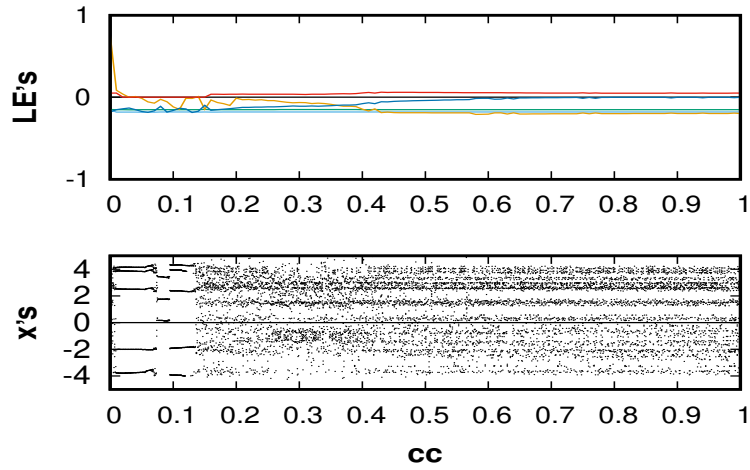


Figure 11: Lyapunov spectra and bifurcation diagram for the mutually coupled Thomas system with nonlinear diffusive coupling with $b = 0.18$ (stable chaotic oscillations)

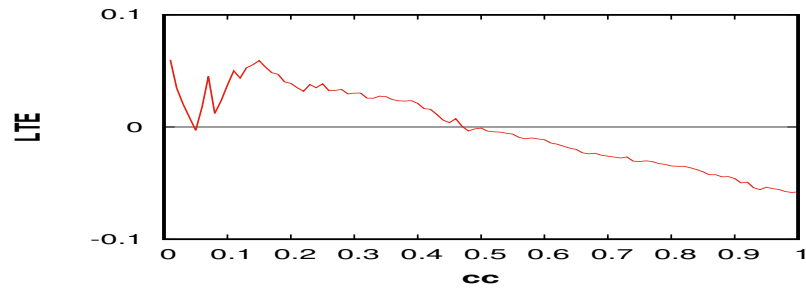


Figure 12: Largest Transverse Lyapunov exponent λ^\perp (LTE) for the mutually coupled Thomas system with nonlinear diffusive coupling with $b = 0.18$ (stable chaotic oscillations)

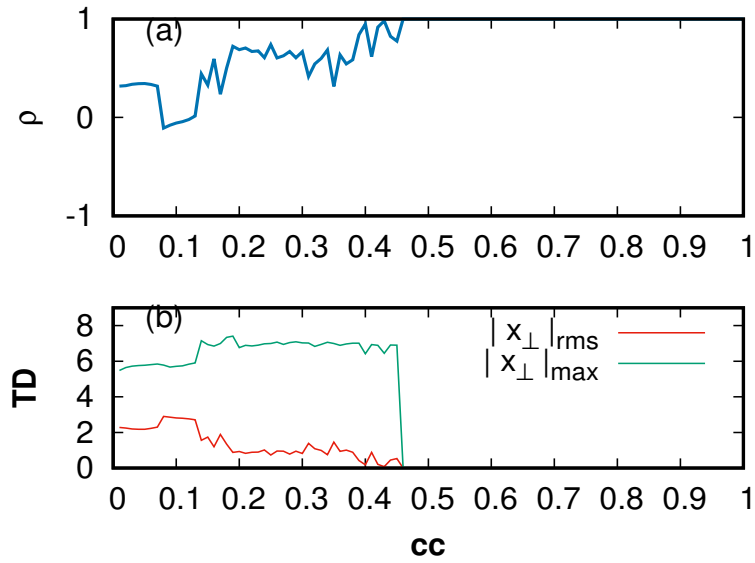


Figure 13: Pearson coefficient (ρ) and Transverse distance (TD) plot for the mutually coupled Thomas system with nonlinear diffusive coupling with $b = 0.18$ (chaotic oscillations)

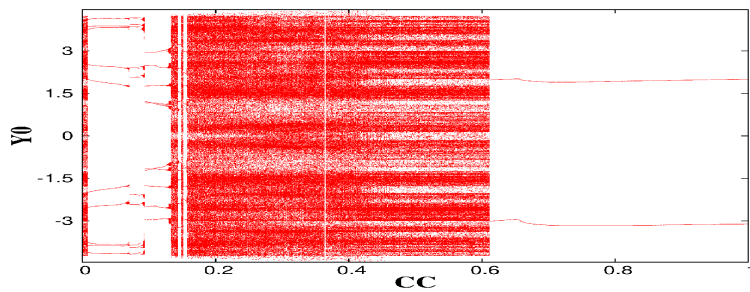


Figure 14: Bifurcation diagram for 1% variation in the initial condition after every cycle of cc with nonlinear diffusive coupling with $b = 0.18$ and transient time 24k(chaotic oscillations)

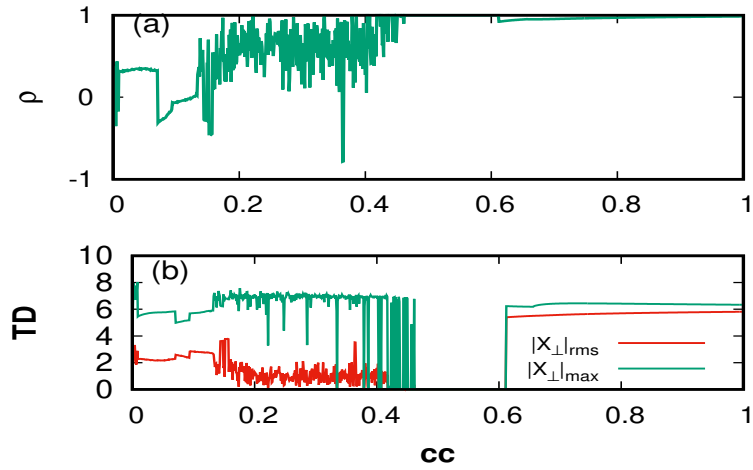


Figure 15: Pearson coefficient (ρ) and Transverse distance (TD) plot for the mutually coupled Thomas system with nonlinear diffusive coupling with $b = 0.18$ and transient time 24k (chaotic oscillations)

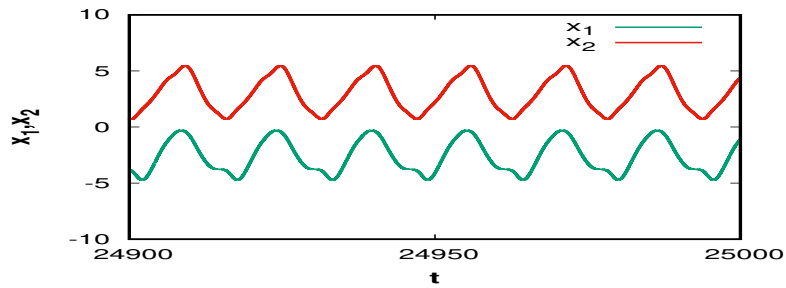


Figure 16: Time series analysis at $cc = 0.7$ for the mutually coupled Thomas system with nonlinear diffusive coupling with $b = 0.18$ and transient time between 24K and 25K (chaotic oscillations)

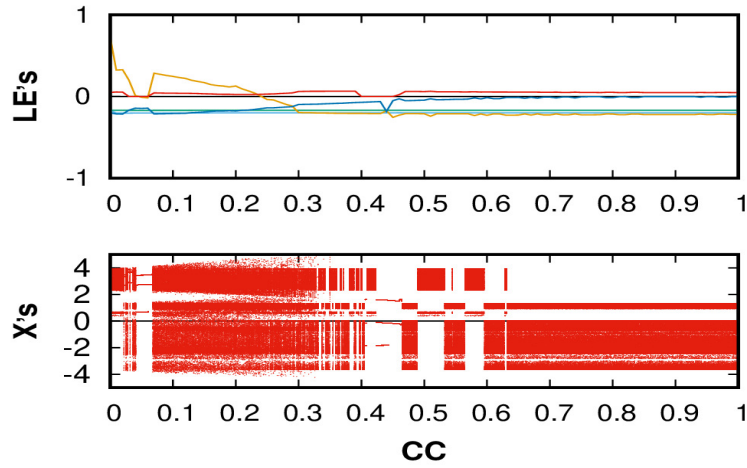


Figure 17: Lyapunov spectra and bifurcation diagram for the mutually coupled Thomas system with nonlinear diffusive coupling with $b = 0.1998$ (stable chaotic but at the border of chaos and quasiperiodic oscillations)

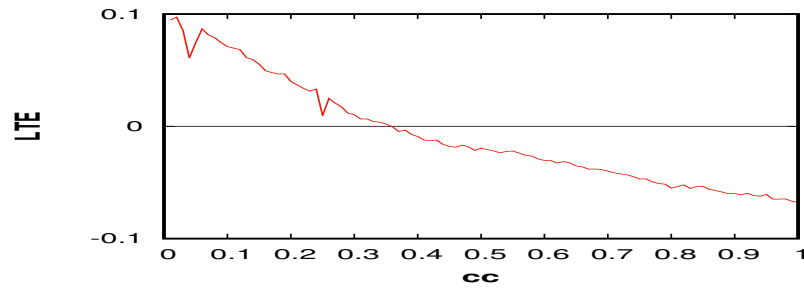


Figure 18: Largest Transverse Lyapunov exponent λ^\perp (LTE) for the mutually coupled Thomas system with nonlinear diffusive coupling with $b = 0.1998$ (stable chaotic but at the border of chaos and quasiperiodic oscillations)

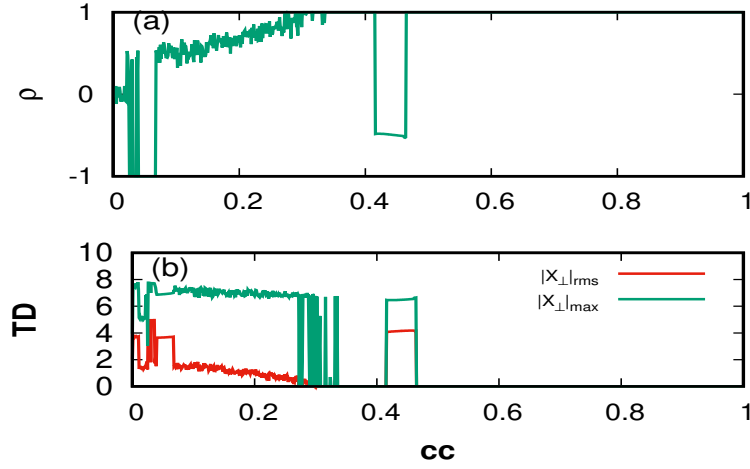


Figure 19: Pearson coefficient (ρ) and Transverse distance (TD) plot for the mutually coupled Thomas system with nonlinear diffusive coupling with $b = 0.1998$ (stable chaotic but at the border of chaos and quasiperiodic oscillations)

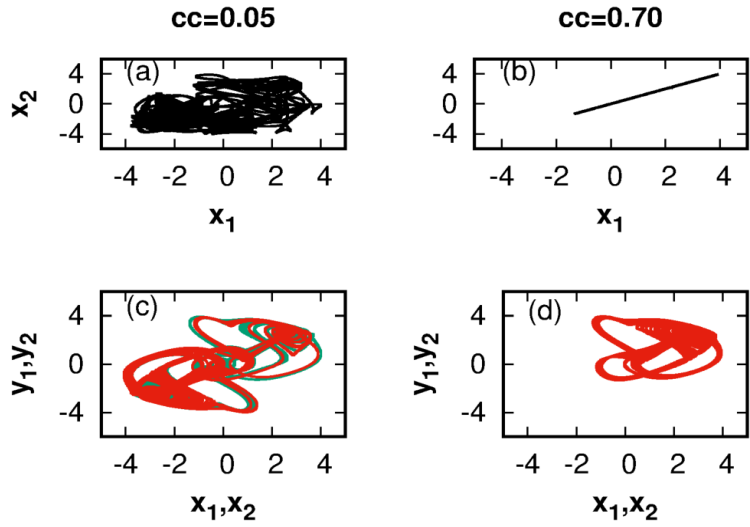


Figure 20: Phase portrait in the case of Non linear Coupling(NLC) with $b = 0.1998$ for two different values of coupling coefficient. Desynchronized state(left panel) and synchronized state(right panel)

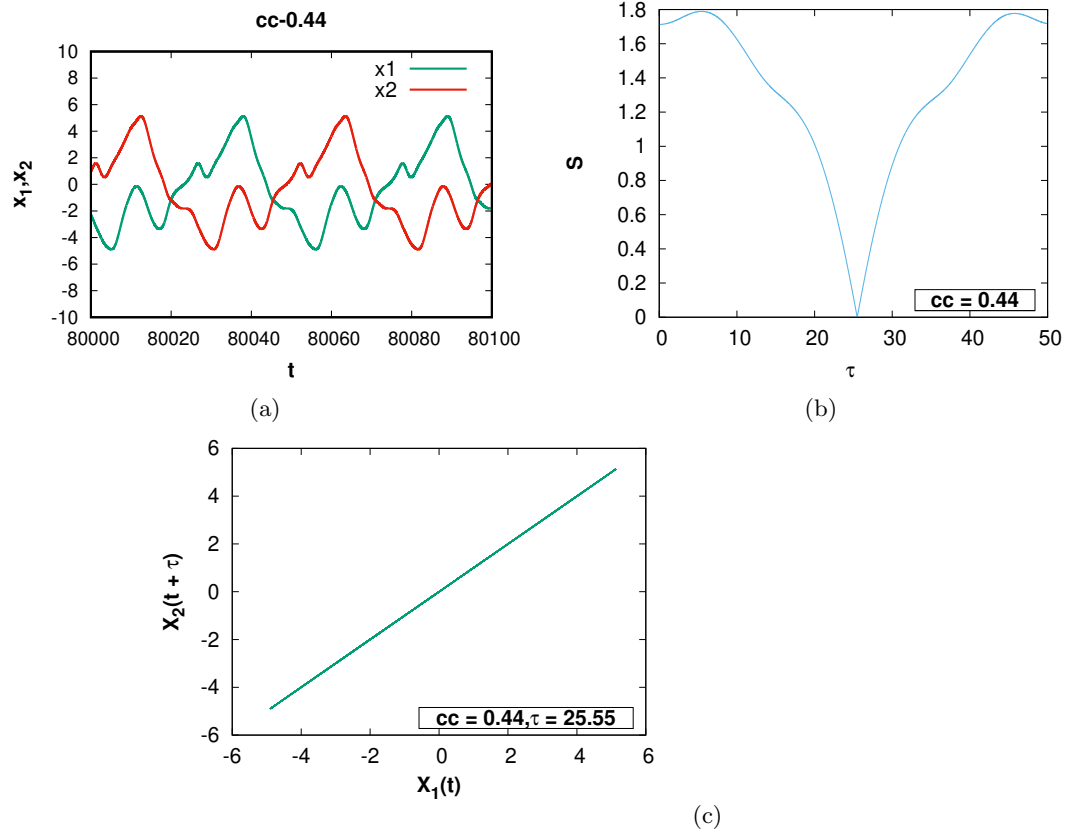


Figure 21: (a)The time series,(b)Similarity index and (c)Lag synchronization for nonlinear coupling with $b = 0.1998$ and $cc = 0.44$

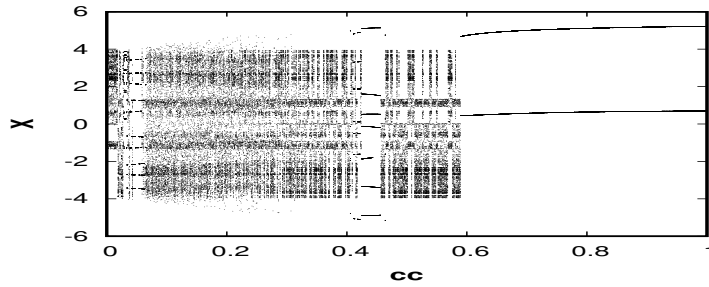


Figure 22: Bifurcation diagram for the mutually coupled Thomas system with nonlinear diffusive coupling with $b = 0.1998$ (chaotic oscillations at the boundary of chaos and quasi-periodic) with 10% variation in initial condition after every cycle of cc , Transient time 80k

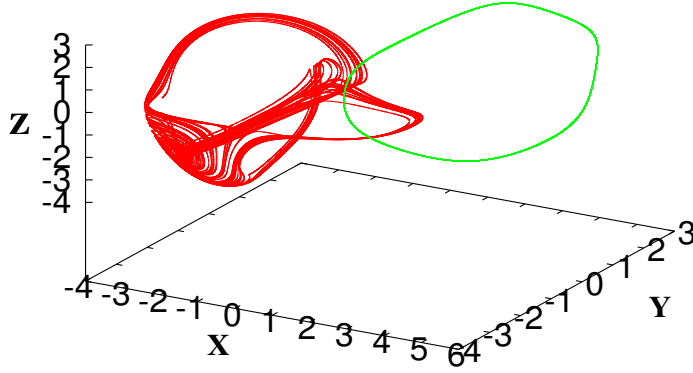


Figure 23: Phase space plot for different initial conditions: with 10% variation (limit cycle) and 1% variation (chaotic) in the initial condition after every cycle of cc with nonlinear diffusive coupling with $b = 0.1998$, Transient time 80k(chaotic oscillations at the boundary of chaos and quasi-periodic)

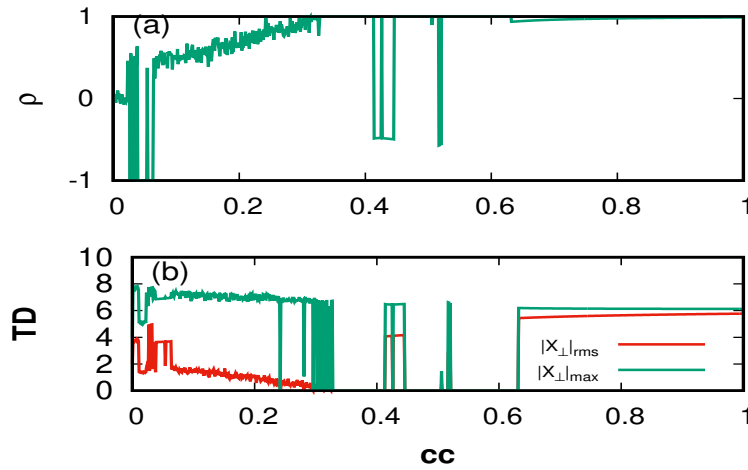


Figure 24: Pearson coefficient (ρ) and Transverse distance (TD) plot for the mutually coupled Thomas system with nonlinear diffusive coupling with $b = 0.1998$ and with 10% variation in the initial condition after every cycle of cc , Transient time 80k

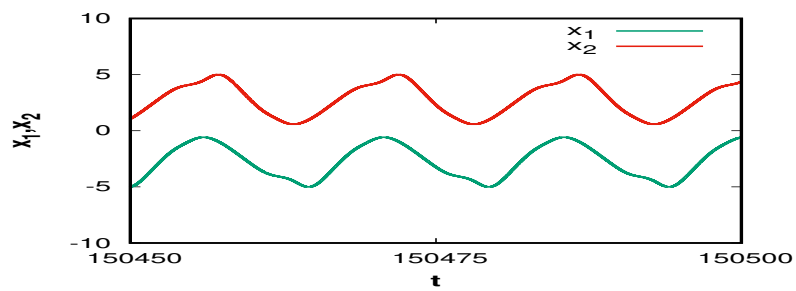


Figure 25: Time series analysis at $cc = 0.7$ for the mutually coupled Thomas system with nonlinear diffusive coupling with $b = 0.1998$ and transient time 150k and second set of initial condition.